Proceedings of 2005 5th IEEE-RAS International Conference on Humanoid Robots

MAC-EYE: a Tendon Driven Fully Embedded Robot Eye *

Dario Biamino, Giorgio Cannata, Marco Maggiali and Alessandro Piazza
Mechatronics and Automatic Control Laboratory (MAC-Lab)
Department of Communications, Computer and Systems Science,
University of Genova
Via Opera Pia 13, 16145, Genova, Italy
{*cannata*}@*dist.unige.it*

***Abstract*— This paper presents a new tendon driven robotic eye. The system has been designed to emulate the actual saccadic and smooth pursuit movements performed by human eyes. The system consists of a sphere (the eye-ball), actuated by four independent tendons driven by four DC motors, integrated in the system. The eye-ball hosts a miniature CMOS color camera and is hold by a low friction support allowing three rotational degrees of freedom. Optical sensors provide feedback to control the correct tendons' tensions during operations. The control of the eye is performed by means of an embedded controller connected to a host computer using CAN bus .**

***Index Terms*— Robot Eye, Listing's Law, Tendon Actuated Robots, Mechatronic Systems, Embedded Control.**

I. Introduction

This paper presents a fully embedded tendon driven robot eye designed to study and emulate the actual movements of a human eye. In fact, eye movements seem to obey to basic laws, whose role for the vision and perception in animals, and implications for the development of intelligent robot and machines are still to be fully understood.

Eye movements have been studied since the mid of the 19^{th} century. However, only during the past 20 years quantitative mathematical models have been proposed, and validated by experiments and clinical test.

Saccadic movements are a very important class of eye motions, [1]. During saccades the eye orientation is determined by a basic principle known as *Listing's Law*, [2], which establishes the amount of eye torsion for each direction of fixation. *Listing's Law* has been experimentally verified on humans and primates [2] – [5], and also found to be valid during other types of eye movements such as *smooth pursuit*, [6]. The geometric properties of *Listing's Law*, [2], [3], [7] – [9], have significant implications on the eye control mechanisms. In fact, on one hand recent anatomical advances, [10] – [14], seem to suggest that the mechanics of the eye plant could play a significant role to implement *Listing's Law*, [9], [15] – [18].

The key problem addressed in this paper is that of designing a robot eye which could generate Listing compatible motions. Furthermore, the system should be used as a component to be embedded in a humanoid system.

*This work is partially supported by Project *Metodi e Algoritmi Innovativi per l'Identificazione e il Controllo Adattativo di Sistemi Tecnologici* granted by the Italian Ministry for University and Research

Many eye-head robots have been designed in the past few years. In many cases these robots have been designed to support and rotate one or more cameras about independent or coupled pan-tilt axes, but little attention has been paid to emulate the actual mechanics of the eye. On the other hand, methodological studies in the area of modelling and control of human-like eye movements have been presented, [19] – [22].

However recent works have focused on the design of embedded mechatronic robot eye systems, [23] – [25]. These systems are very compact and often self-contained, and could be used as components for integrating head-eye robots. Pongas et al., [25], have developed a single DOF mechanism which actuates a CMOS micro-camera embedded in a spherical support. The system has a single degree of freedom (DOF), and the spherical shape of the eye is a purely aesthetical detail. However, the mechatronic approach adopted to the design has addressed many important engineering issues and has led to a very integrated and clever system.

In the prototype developed by Albers et al., [24], the design is more *humanoid*. The robot consists of a sphere supported by *slide bearings* and moved by a stud constrained by two gimbals. This design exploits the spherical shape of the eye, however, the two DOFs design proposed does not seems to meet the motion requirements specified by *Listing's Law*.

The goal of this paper is to investigate the possibility of designing a robot eye with kinematics and actuation similar to those of the human eye. In particular, we tried to exploit the spherical shape of the eye and to study the feasibility of a tendon based actuation mechanism which could implement *Listing's Law*. The robot presented in this paper consists of a sphere hold by a low friction support. Four independent tendons, actuated by four DC motors, allow the proper rotation of the eye. A suitable placement of the insertion points of the tendons on the eye-ball, as well as their routing to the motors have been investigated. Simulations have shown that the proposed configuration meets the motion requirements specified by *Listing's Law*.

The structure of the paper is the following. In section II, we will present *Listing's Law* and its mechanical and control implications. In section III the eye model used for the implementation of the robot and simulation results will be shortly discussed. Then, in section IV a detailed description of the robot eye components and subsystems will be given.

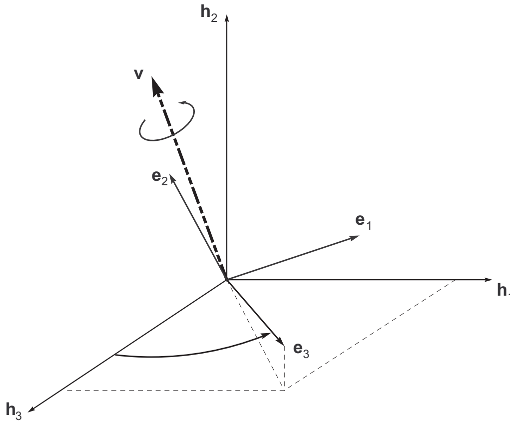

Fig. 1. Geometry of Listing compatible rotations.

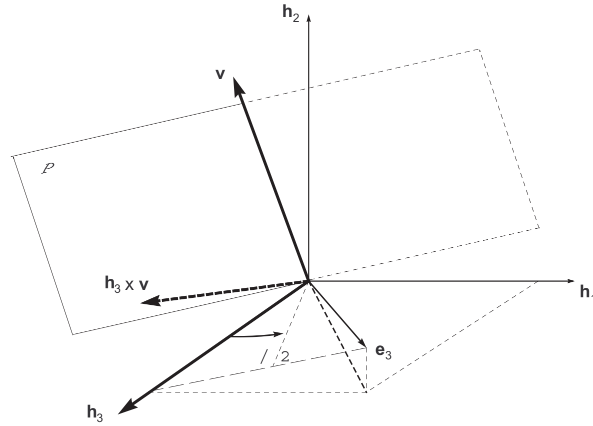

Fig. 2. Half angle rule geometry.

II. Saccadic Movements and Listing's Law

Eye movements have the goal of optimizing visual perception. The way the eyes change their orientation may affect our perception of the world. In turn, it is widely accepted that visual feedback, as well as other sensory feedback (e.g. from vestibular system), plays a main role in stimulating eye movements. Therefore, it is not surprising that to different vision strategies correspond significantly different types of eye motions. During saccades for instance the major goal is probably that of reaching as fast as possible a target fixation direction, while during VOR the main goal is to keep stable the image on the retina despite possible *external disturbances*.

In the following we will focus on saccadic motions, and to *Listing's Law* which specifies the eye's orientation during saccades.

Listing's Law. There exists a specific eye orientation with respect to the head, called *primary position*. During saccades any physiological eye orientation, with respect to the *primary position*, can be described by a unit quaternion q whose (unit) rotation axis, $\mathbf{v}$, always belongs to a head fixed plane, $\mathcal{L}$. The normal to plane $\mathcal{L}$ is the eye's direction of fixation at the *primary position*.

Let $\{\mathbf{h_1}, \mathbf{h_2}, \mathbf{h_3}\}$ and $\{\mathbf{e_1}, \mathbf{e_2}, \mathbf{e_3}\}$ be a head fixed and eye fixed reference frames respectively. Without loss of generality we can assume $\mathbf{h_3}$ to be the fixation axis at the *primary position*, then $\mathcal{L} = span\{\mathbf{h_1}, \mathbf{h_2}\}$. Fig. 1 shows the geometry of Listing compatible rotations.

From the kinematic point of view, during saccades, at any time t, the rotation of the eye can be conveniently described by a unit quaternion:

$$q = \left(\cos\frac{\theta}{2}, \mathbf{v}\sin\frac{\theta}{2}\right), \tag{1}$$

where $\mathbf{v} \in \mathcal{L}, |\mathbf{v}| = 1$, and θ is the amount of rotation with respect to the *primary position*. The derivative of (1) is:

$$\dot{q} = \frac{1}{2}\,\tilde{\omega}\;q, \tag{2}$$

where quaternion $\tilde{\omega} = (0, \omega)$ and ω is the angular velocity of the eye. By expanding (2) we obtain:

$$\dot{q} = \frac{1}{2}\left((\omega\cdot\mathbf{v})\sin\frac{\theta}{2}, \omega\cos\frac{\theta}{2} + (\omega\times\mathbf{v})\sin\frac{\theta}{2}\right). \tag{3}$$

In order to guarantee the condition $\mathbf{v} \in \mathcal{L}$, we must have $\dot{\mathbf{v}} \in \mathcal{L}$, for any ω, then from (3) the following equality must hold:

$$\mathbf{h_3}\cdot\left[\omega\cos\frac{\theta}{2} + (\omega\times\mathbf{v})\sin\frac{\theta}{2}\right] = 0. \tag{4}$$

Expression (4) leads to the formula:

$$(\omega\cdot\mathbf{h_3}) = \omega\cdot(\mathbf{h_3}\times\mathbf{v})\tan\frac{\theta}{2}, \tag{5}$$

stating that two components of ω are constrained each other, while the third one (directed along the axis $\mathbf{v}$) can be arbitrarily fixed. In particular, from (5) we obtain that the angular velocity of the eye is constrained to a plane $\mathcal{P}_\omega$ passing through $\mathbf{v}$, and whose normal forms an angle of $\frac{\theta}{2}$ with axis $\mathbf{h_3}$, see fig. 2. This property is directly implied by *Listing's Law*, and is usually called *half angle rule*, [8].

The *half angle rule* has important implications. First of all, although *Listing's Law* implies zero torsion of the eye, the eye's angular velocities may have a torsional component (i.e. a component directed along axis $\mathbf{h_3}$. The second, and most important remark, is that ω is constrained to lay on a moving plane, $\mathcal{P}_\omega$ which is not fixed to the head, neither to the eye for its dependency from $\mathbf{v}$ and $\frac{\theta}{2}$. This fact poses important questions related to the control mechanisms required to implement the *Listing's Law*.

The evidence of soft tissue, called *soft pulleys*, within the orbit, [10] – [14], constraining the extra ocular muscles (EOMs), has suggested that the mechanics of the eye plant could have a significant role in the implementation of *half angle rule* and *Listing's Law*, [15] – [18], although counterexamples have been presented in the literature, [26], [27].

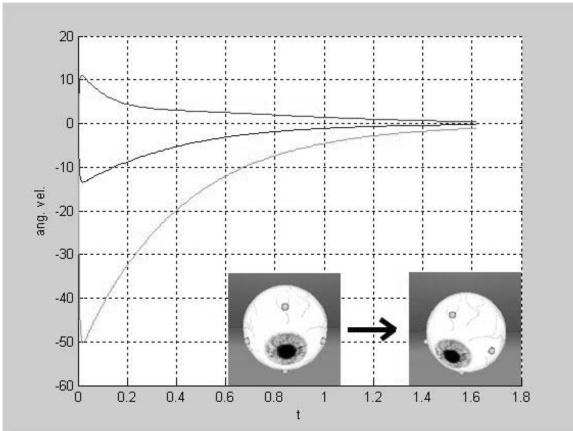

Fig. 3. Components of angular velocity during a saccade from a secondary to a tertiary position.

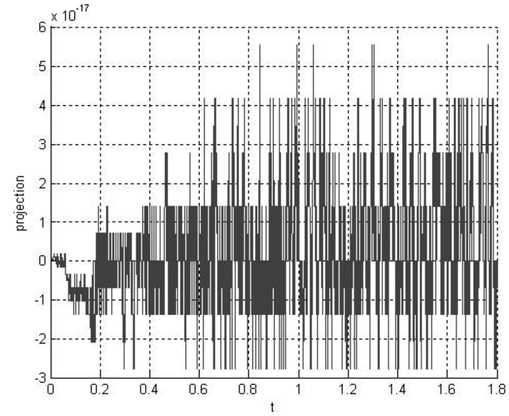

Fig. 4. Component of the rotation vector off the *Listing's Plane*.

III. Robot Eye Model

The basic principles discussed in the previous section represent the basis for the development of the robot eye presented in the following.

The robot eye-ball has been modelled as an homogeneous sphere with 3 rotational DOFs, and actuated by the action of EOMs, [28]. Following the rationale of [9], and [15] we have considered only 4 EOMs, instead of 6, assuming negligible the role of the upper and lower obliqui muscles. The EOMs have been modelled as thin wires of fixed length, as in [15], connected on one side to the eye-ball and to springs at the second end.

Starting from the insertion points on the eye-ball, the tendons are routed to fixed *point-wise* pulleys placed on the rear of the eye-ball. The tendons follow the shortest path from their insertion points to the corresponding pulleys, [12]. Therefore, for any given eye orientation it is quite simple to compute the motion of the tendons and the resulting actuation force due to the springs.

Simulations have shown that the relative position of the insertion points and the position of the pulleys is critical on one hand for the stability of the eye and on the other to achieve realistic motions, [29], [30]. In particular, it has been shown, [29], that a symmetric configuration of the insertion points and of the pulleys with respect to the center of the eye-ball ensures Listing compatible rotations for any pattern of forces applied by the tendons. Fig. 3 shows the components of the angular velocity for a generic saccade from a secondary to a tertiary position; fig. 4 show the amount of violation of *Listing's Law*, i.e $(\mathbf{h_3} \cdot \mathbf{v})$.

IV. MAC-EYE Design and Implementation

The design of the MACEYE robot has been based on the main specification discussed in previous sections. The robot eye consists of various modules shortly described in the following.

A. The Eye-Ball

The eye ball is a precision PTFE sphere having a diameter of $38.1mm$ $(1.5in)$. The sphere has been CNC machined to host a commercial CMOS camera, a suspension spring, and to route the power supply and video signal cables to the external electronics. A frontal flange is used to allow the connection of the tendons and to support miniature screws required to calibrate the position of the camera. On the flange is eventually placed a spherical cover purely for aesthetical reasons. Fig. 5 and fig. 6 show the exploded view and the actual eye-ball.

B. The Eye-Ball Support

In order to support the eye ball it has been designed the part shown in fig. 7. The part is made of PTFE and together with the eye-ball forms a sort of spherical sliding bearing. As shown in fig. 8, an external (rigid) flange stiffens the structure and provides appropriate pre-load.

The role of the flange is also that of ensuring the appropriate routing of the tendons from their insertion points on the eye-ball to the actuation motors. As discussed in section III, the tendons' routing must be constrained by some sort of pulley. The ideal solution of a *point-wise pulley* has been actually approximated as shown in fig. 9.

Starting from the motors, and for any (admissible) eye orientation each tendon follows a common path (axis $\mathbf{c}$ in

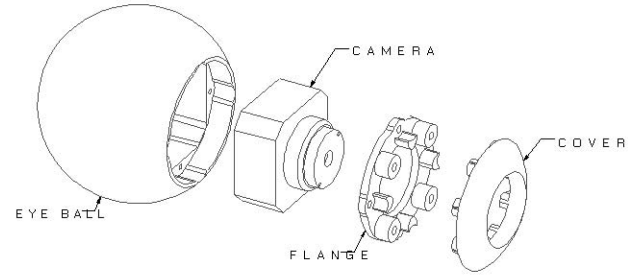

Fig. 5. Exploded view of the eye-ball (internal camera support spring not shown)

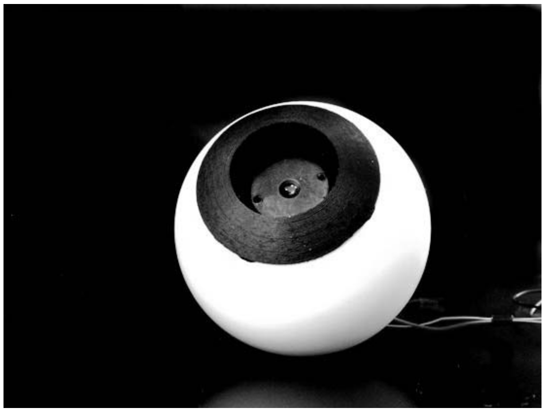

Fig. 6. Assembled eye-ball (camera cables shown in background)

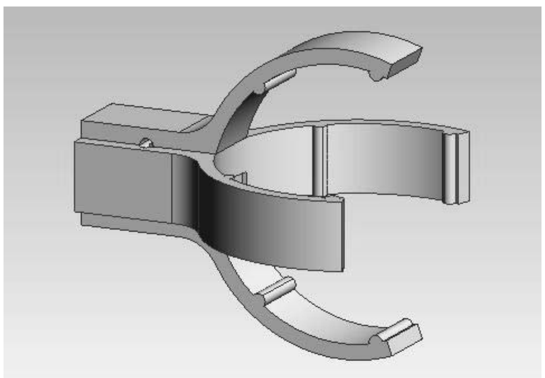

Fig. 7. CAD model of the eye-ball support.

fig. 9). Then, each tendon is assumed to be routed through a pulley which can tilt about axis **c**. The resulting path for each tendon is then planar for each eye orientation. In order to implement this model, we have considered the surface obtained by the envelope of the *tilting* pulleys, for any possible Listing compatible eye orientation. This surface has been machined on the supporting flange leading to the structure shown in fig. 10. This solution implies the sliding of the tendons, but significantly simplify the implementation.

C. The Eye Body

The body of the MAC-EYE robot consists of four segments (including the flange previously discussed), made of *acetal homopolymer resin*, designed to embed the four DC motors required to actuate the eye, and the sensors required to control the tension of the tendons. All cables coming from the eye, the motors and the embedded sensors, as well as the tendons are routed within the eye body. Fig. 11 shows the robot MAC-EYE assembled; the four internal DC motors (Faulhaber model 1524, including 1:11 gearhead model 15/6) are fixed on the back cover of the body as shown in fig. 12.

The whole structure weighs about $350g$, has an external diameter of $50mm$ and is $100mm$ long (including eye-ball and back motor pulleys).

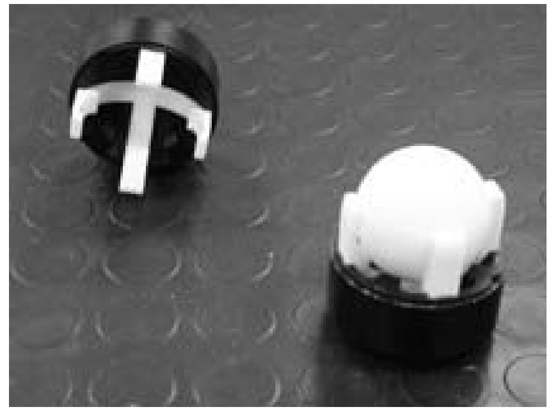

Fig. 8. The eye-ball and its support flange.

D. Sensors

The only sensors used to control the movements of the eye are the encoders of the DC motors and the sensors required to control the tendons' tensions. The use of visual feedback by means of the on board CMOS camera is not part of the present discussion.

1) Encoders: The encoders are the main source of feedback to control eye movements. Encoder resolution is $1024ppr$; by taking into account account the gearmotor reduction ratio $(11.8:1)$, the motor pulley to eye-ball reduction ratio $(38.1:6)$, the *nominal* eye orientation accuracy is about of $0.005deg$.

2) Tension Sensors: The eye is actuated by four tendons made of low friction nylon cables (diameter $0.25mm$). In order to avoid the slackness of the tendons optical tension sensors have been designed to implement a tension closed-loop control, fig. 13. The sensor is formed by an infrared led/photodiode couple separated by a mobile *shutter*, pre-loaded with a phosphore-bronze spring. As shown in fig. 14 the tension of the tendon counter-balances the pre-load force thus varying the amount of IR radiation received.

The sensor output is the current generated by the photodiode accordingly to the following equation:

$$I_p = k_p \gamma(f) E_0, \tag{6}$$

where I_p is the current generated by the photodiode, k_p is a characteristic parameters of the photodiode, E_0 is the IR radiation emitted by the led, and $\gamma(f)$ is a monotonic

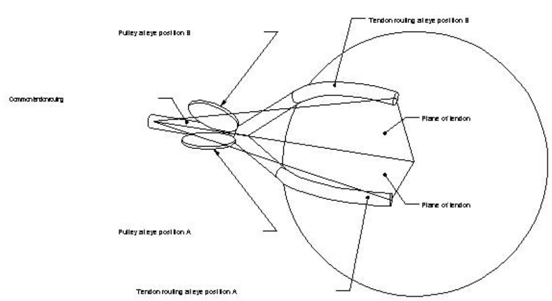

Fig. 9. Sketch of the tendon's paths, showing the tilting of the routing pulley (tendons and pulleys diameters not to scale).

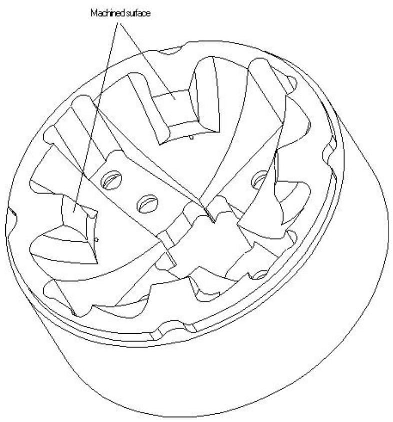

Fig. 10. Detail of the flange supporting the eye-ball.

Fig. 11. MAC-EYE assembled (without camera)

Fig. 12. Four DC motor actuate the tendons; pulleys (barely visible here) route the tendons towards the eye-ball.

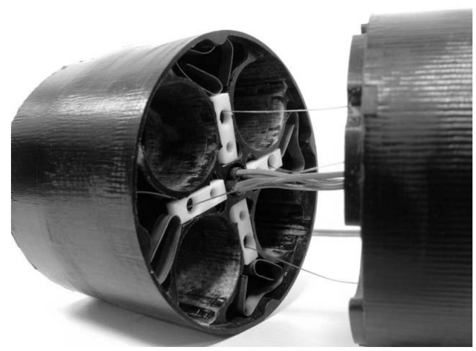

Fig. 13. Implementation of the embedded tendons' tension sensors. The picture shows the *shutter* and the spring, cables and tendons.

non- linear function of the tendon's tension depending on the system geometry. Each sensor is calibrated during assembly and a look-up table is used to map its current to tension characteristic.

E. Control Architecture

The control architecture is implemented as a two level hierarchical system. A high level digital control module currently implements a PI-type regulation of the path lengths of the tendons. This control module is implemented on a PC, and is currently used to compare the experimental results with the simulations (where extraocular muscles have been modelled as springs). An open loop geometric model of the eye plant and tendon's routing has been implemented to generate admissible tendons' lengths.

At low level a custom embedded controller implements the actual motor control loops. The low level controller consists of 4 slave micro-controllers coordinated by a master one, fig. 15.

Each slave controller is interfaced with a single DC motor driver (PWM amplifier), and encoder, and measures the corresponding tendon's tension. The control scheme, currently implemented, is a PI-type motor velocity control loop in parallel with a P-type tension control loop, both running at $1.25KHz$. Using this control scheme the eye is *actively* back-drivable, i.e. the eye position can be set *by hand*.

The master controller implements the real-time communications with the high level control modules through CAN bus (at $125Hz$ rate), and synchronizes the operations of the slave controllers using a multiplexed high speed serial link .

V. CONCLUSIONS

In this paper we have presented a new tendon driven fully embedded robot eye called MAC-EYE. This prototype has a kinematic and actuation structure which emulate the characteristics of a human eye. In particular, the study has focused on a design which meets the motion constraints imposed by *Listing's Law*. Simulative analysis has driven the actual robot implementation.

Finally, a complete stereoscopic system is shown in fig. 16.

ACKNOWLEDGMENT

The authors wish to thank Mr. Claudio Beretta and Mr. Giorgio Carlini for their invaluable support during the construction of the prototype of the robot MAC-EYE.

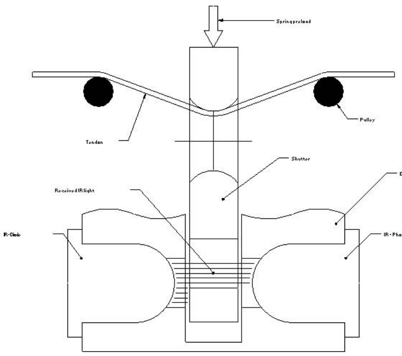

Fig. 14. Sketch of the tension sensor (not to scale).

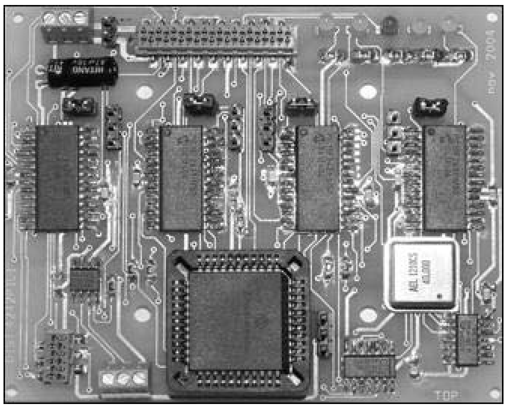

Fig. 15. The embedded real-time controller. The board has dimensions of 69×85 ^{2} to be integrated with the eye

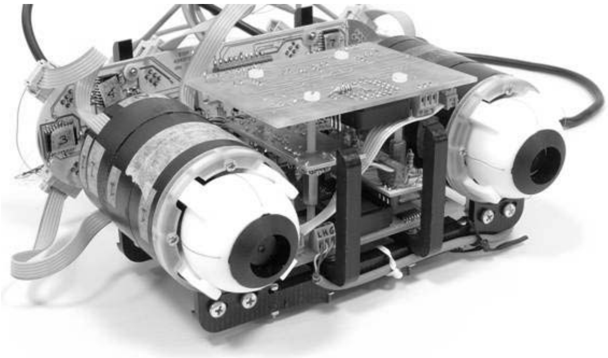

Fig. 16. Complete stereoscopic robot system

References

[1] W. Becker, "Eye Movements," in ,Carpenter, R.H.S. ed., Macmillan 1991, pp. 95-137.

[2] D. Tweed, T. Vilis, "Implications of Rotational Kinematics for the Oculomotor System in Three dimensions," The Journal of Neurophysiology, vol. 58, no.4, pp. 832-849, Oct. 1987.

[3] D. Tweed, T. Vilis, "Rotation Axes of Saccades," Ann. N. Y. Acad. Sci., vol. 545, pp. 128-139, 1988.

[4] D. Tweed, T. Vilis, "Geometric relations of eye position and velocity vectors during saccades," Vision. Res., vol. 30, n. 1, pp. 111-127, 1990.

[5] J. M. Furman adn R. H. Schor, "Orientation of Listing's plane during static tilt in young and older human subjects," Vision Res., vol. 43, pp. 67-76, 2003.

[6] D. Straumann, D. S. Zee., D. Solomon and P. D. Kramer, "Validity of Listing's law during fixations, saccades, smooth pursuit eye movements, and blinks," Exp. Brain Res., vol. 112, pp. 135-146, 1996.

[7] D. Tweed, T.Haslwanter and M. Fetter, "Optimizing Gaze Control in Three Dimensions," Science, vol. 281, Aug. 1998.

[8] T. Haslwanter, "Mathematics of Three-dimensional Eye Rotations," Vision Res., vol. 35, pp. 1727-1739, 1995.

[9] T. Haslwanter, "Mechanics of Eye Movements: Implications of the "Orbital Revolution," Ann. N. Y. Acad. Sci., vol. 956, pp. 33-41, 2002.

[10] L. Koornneef, "The first results of a new anatomical method of approach to the human orbit following a clinical enquiry," Acta Morphol Neerl Scand, vol. 12, n. 4, pp. 259-282, 1974.

[11] J. M. Miller, "Functional anatomy of normal human rectus muscles," Vision Res., vol. 29, pp. 223-240, 1989.

[12] J. L. Demer, J. M. Miller,V. Poukens,H. V. Vinters and B.J. Glasgow, "Evidence for fibromuscular pulleys of the recti extraocular muscles," Investigative Ophthalmology and Visual Science, vol. 36, pp. 1125-1136, 1995.

[13] R. A. Clark, J.M. Miller, J. L. Demer," Three-dimensional Location of Human Rectus Pulleys by Path Inflection in Secondary Gaze Positions," Investigative Ophthalmology and Visual Science, vol. 41, pp. 3787-3797, 2000.

[14] J. L. Demer, S. Y. Ho, V. Pokens, "Evidence for Active Control of Rectus Extraocular Muscle Pulleys," Invest. Ophtalmol. Visual Sci., vol. 41, pp. 1280-1290, 2000

[15] A. R. Koene, C.J. Erkelens, "Properties of 3D rotations and their relation to eye movement control," Biol. Cybern., vol. 90, pp. 410-417, Jul. 2004.

[16] J. Porrill, P. A. Warren, P. Dean, "A simple control law generates Listing's positions in a detailed model of the extraocular muscle system," Vision Res., vol. 40, pp. 3743-3758, 2000.

[17] C. Quaia, L. M. Optican, "Commutative Saccadic Generator Is Sufficient to Control a 3D Ocular Plant With Pulleys," The Journal of Neurophysiology, vol. 79, pp. 3197-3215, 1998.

[18] T. Raphan, "Modeling Control of Eye Orientation in Three Dimensions. I. Role of Muscle Pulleys in Determining Saccadic Trajectory," The Journal of Neurophysiology, vol. 79, pp. 2653-2667, 1998.

[19] P. Lockwood-Cooke, C. F. Martin and L. Schovanec, "A Dynamic 3-d Model of Ocular Motion," Proceedings of the 38th Conference of Decision and Control, Phoenix, Dec.1999.

[20] A. D. Polpitiya and B. K. Ghosh, "Modelling and control of eye-movement with muscolotendon dynamics," Proceedings of the American Control Conference, pp. 2313-2318, Anchorage, May, 2002.

[21] A. D. Polpitiya and B. K. Ghosh, "Modeling the Dynamics of Oculomotor System in Three Dimensions," Proceedings of the Conference on Decision and Control, pp. 6418-6422, Maui,Dec. 2003

[22] A. D. Polpitiya, B. K. Ghosh, C. F. Martin and W. P. Dayawansa, "Mechanics of the Eye Movement: Geometry of the Listing Space," Proceedings of the American Control Conference, 2004.

[23] J. Gu, M. Meng, A. Cook and M. G. Faulkner, "A study of natural movement of artificial eye plant ," Robotics and Autonomous System, vol. 32, pp. 153-161, 2000.

[24] A. Albers, S. Brudniok, W. Burger, "The Mechanics of a Humanoid," Proceedings of Humanoids 2003, Karlsruhe, Germany, 2003.

[25] Pongas, D., Guenter, F., Guignard, A. and Billard, A. "Development of a Miniature Pair of Eyes With Camera for the Humanoid Robot Robota. IEEE-RAS/RSJ International Conference on Humanoid Robots, 2004.

[26] K. Hepp, "Oculomotor control: Listing's law and all that," Current Opinion in Neurobiology, vol. 4, pp. 862-868, 1994.

[27] A. M. F. Wong, D. Tweed and J. A. Sharpe, "Adaptive Neural Mechanism for Listing's Law Revealed in Patients with Sixth Nerve Palsy," Investigative Ophtalmology and Visual Science, vol. 43, n. 1, pp. 112-118, Jan. 2002

[28] G. K. Hung, "Models of Oculomotor Control," World Scientific Pub. Co. Inc., 2001

[29] G. Cannata, "Notes on Listing's Law Implementation," unpublished.

[30] D. Biamino, A. Piazza, "Studio Progetto e Realizzazione di una Coppia di Occhi Robotici con Sistema di Controllo Embedded," Master Degree Thesis, Faculty of Engineering, University of Genova, 2005.